Ionic rotational branching ratios in resonant enhanced multiphoton ionization of NO via the $A\,^2\Sigma^+(3s\sigma)$ and $D\,^2\Sigma^+(3p\sigma)$ states

H. Rudolph
Arthur Amos Noyes Laboratory of Chemical Physics, California Institute of Technology, Pasadena, California 91125

S. N. Dixit
Lawrence Livermore National Laboratory, L-401, P. O. Box 808, Livermore, California 94550

V. McKoy
Arthur Amos Noyes Laboratory of Chemical Physics, California Insitute of Technology, Pasadena, California 91125

W. M. Huo
NASA-Ames Research Center MS230-3, Moffett Field, California 94035

(Received 21 August 1987; accepted 29 September 1987)

We present the results of *ab initio* calculations of the ionic rotational branching ratios in NO for a (1 + 1) REMPI (resonant enhanced multiphoton ionization) via the $A\,^2\Sigma^+(3s\sigma)$ state and a (2 + 1) REMPI via the $D\,^2\Sigma^+(3p\sigma)$ state. Despite the atomic-like character of the bound $3s\sigma$ and $3p\sigma$ orbitals in these resonant states, the photoelectron continuum exhibits strong l mixing. The selection rule $\Delta N + l =$ odd ($\Delta N \equiv N_+ - N_i$) implies that the peaks in the photoelectron spectrum corresponding to $\Delta N =$ odd ($\pm 1, \pm 3$) are sensitive to even partial waves while those corresponding to even ΔN probe the odd partial waves in the photoelectron continuum. Recent experimental high resolution photoelectron studies have shown a strong $\Delta N = 0$ peak for ionization via the $A\,^2\Sigma^+$ and the $D\,^2\Sigma^+$ states, indicating a dominance of odd-l partial waves. While this seems natural for ionization out of the $3s\sigma$ orbital, it is quite anomalous for $3p\sigma$ ionization. Based on extensive bound calculations, Viswanathan *et al.* [J. Phys. Chem. **90**, 5078 (1986)] attribute this anomaly to a strong l mixing in the electronic continuum caused by the nonspherical molecular potential. We have performed *ab initio* calculations of the rotational branching ratios and compared them with the experimental results. The electronic continuum shows a significant p-wave component which leads to the large $\Delta N = 0$ peak in both cases. Calculations are performed for both rotationally "clean" and "mixed" branches. The relative heights of the peaks are very sensitive to the photoelectron kinetic energy for the $D\,^2\Sigma^+$ state and less so for the $A\,^2\Sigma^+$ state. This is a direct consequence of the l mixing in the continuum.

I. INTRODUCTION

The technique of resonant enhanced multiphoton ionization (REMPI) combined with high resolution photoelectron spectroscopy (PES) has in recent years proven useful in elucidating the finer dynamical details of the photoionization of smaller molecules.[1-5] The rotationally resolved photoelectron spectra display highly detailed information concerning both the intermediate resonant state and the photoionization dynamics. The limitations on the resolution of the photoelectron energy detection ($\approx$5 meV) have restricted rotationally resolved PES studies to H_2[6-9] and with some difficulty to NO.[10-16] New techniques involving threshold photoelectron detection have achieved rotational resolution for relatively low rotational quantum numbers.[17] In a series of recent papers[14-16] Reilly and co-workers have demonstrated very detailed rotationally resolved photoelectron spectra via the $A\,^2\Sigma^+$, $D\,^2\Sigma^+$, and the $C\,^2\Pi$ state of NO. Their spectral resolution (3 meV at best) permits a separation of the rotational structure for medium to high values of J due to the relatively large rotational constant of the NO^+ ion ($B_e \cong 2\,cm^{-1}$). The (1 + 1) REMPI via the $A\,^2\Sigma^+$ state shows a pronounced $\Delta N = 0$ peak with smaller, but significant, $\Delta N = \pm 2$ peaks. The (2 + 1) REMPI via the $D\,^2\Sigma^+$ state shows a significant $\Delta N = 0$ signal in addition to the expected $\Delta N = \pm 1, \pm 3$ peaks. While the observed rotational branching ratios for the $A\,^2\Sigma^+$ state[14] could be rationalized on the basis of an atomic-like model, the $\Delta N = 0$ peak in the $D\,^2\Sigma^+(3p\sigma)$ photoelectron spectra is not consistent with such a model. The almost pure p character (98%)[15,18] of the $D\,^2\Sigma^+$ state would predict a predominant s- or d-wave character of the continuum, giving rise to a dominant $\Delta N = \pm 1$ or ± 3 signal.[19] On the basis of very extensive bound state calculations Viswanathan *et al.*[15] suggested, that the $\Delta N = 0$ peak must be due to odd partial wave character in the electronic continuum arising from the nonspherical nature of the molecular potential.

Recently, we reported calculated rotationally resolved PES for (1 + 1) REMPI via the $A\,^2\Sigma^+$ state[20] as well as for the (2 + 1) REMPI via the $D\,^2\Sigma^+$ state.[21] The results agreed quite well with experimental data.[15] Our results for the $D\,^2\Sigma^+$ state show significant intensity in the $\Delta N = 0$

 0021-9606/88/020637-05$02.10

peak, thus confirming the suggestion of Viswanathan *et al.*[15] that the $\Delta N = 0$ peaks were due to final state interactions. Due to their Rydberg character, the ion cores of the A and D states should be very similar. The photoelectron continuum of these ion cores, should also be similar in these two cases. This suggests that differences in the PES for REMPI via these two states are a consequence of the probing of different angular momentum components of the continuum through the photoelectron matrix element in these two cases. To analyze this feature, we have performed additional PES calculations for rotationally clean and mixed branches and for a range of photoelectron kinetic energies. The results presented in Sec. III demonstrate the importance of the molecular nature of the continuum and stress the necessity for a proper treatment of it.

II. THEORY

The general theory of molecular REMPI processes has been described previously[22] and only details pertaining to this particular application will be given here. The $(n+m)$ REMPI process can be thought of conceptually as an n-photon absorption from an initially unaligned (all M_J levels equally populated) ground state, to a resonant intermediate state, followed by an m-photon ionization out of this aligned intermediate state,

$$\mathrm{NO}\ X\,^2\Pi(v'',J'') \xrightarrow{h\nu} \mathrm{NO}^*A\,^2\Sigma^+(v',J',N')$$

$$\xrightarrow{h\nu} \mathrm{NO}^+X\,^1\Sigma^+(v^+,J^+=N^+)+e^-(\mathbf{k}), \tag{1a}$$

$$\mathrm{NO}\ X\,^2\Pi(v'',J'') \xrightarrow{2h\nu} \mathrm{NO}^*D\,^2\Sigma^+(v',J',N')$$

$$\xrightarrow{h\nu} \mathrm{NO}^+X\,^1\Sigma^+(v^+,J^+=N^+)+e^-(\mathbf{k}). \tag{1b}$$

REMPI out of each M_J level of the initial state can be treated as an independent channel in the case of linearly polarized photons and in the absence of M_J mixing terms (collisions, etc.). For weak field excitations, the population ρ_{ii} of the intermediate state can be calculated using lowest-order perturbation theory. For the single photon Π–Σ excitation of the A state, ρ_{ii} is given by

$$\rho_{ii} \propto \begin{pmatrix} J' & 1 & J'' \\ -M_{J'} & 0 & M_{J'} \end{pmatrix}^2 A \tag{2a}$$

and for the two-photon Π–Σ excitation of the D state

$$\rho_{ii} \propto \begin{pmatrix} J' & 2 & J'' \\ -M_{J'} & 0 & M_{J'} \end{pmatrix}^2 B, \tag{2b}$$

where J' and J'' are defined in Eq. (1). For a Π–Σ transition the constants A and B can be taken to be independent of the electronic transition moments.[23] For relative ρ_{ii} in pure branches (only one J' state) A and B can be disregarded as well. However, for mixed branches (two J' states corresponding to $N' \pm 1/2$) the relative weights A and B can be calculated using the description of Earls[24] and of Halpern,[23] respectively. The photoelectron angular distribution $P(\theta)$, where θ is the angle with respect to the polarization vector of the radiation, can then be written as

$$\frac{dP(\theta)}{dt} \propto \sum_{\text{branches}} \sum_i \Gamma_i(\theta)\cdot\rho_{ii}. \tag{3}$$

Γ_i is the ionization width for the particular M_J level of the intermediate state and involves sums of the square of the transition matrix elements, i.e.,

$$r_{fi}^{\lambda\mu} = \sum_{l',l_0} \langle \Psi_{kll'}(r)\,Y_{l'\lambda}(\hat{r}') | r Y_{1\mu}(\hat{r}') | \Phi_{il_0}(r)\,Y_{l_0 0}(\hat{r}') \rangle \tag{4}$$

as given by Eq. (13) of Ref. 20. The $r_{fi}^{\lambda\mu}$ matrix elements are evaluated using photoelectron continuum orbitals obtained by the variational Schwinger method and the single-center expansion technique.[25] The photoelectron Hartree–Fock continuum wave function is determined in the frozen-core approximation using the intermediate state's $(N-1)$ electron core for the A state and the fully-relaxed ion core for the D state. As shown later, the core of the A state is nearly identical to the fully relaxed ion core due to the diffuse nature of the Rydberg 6σ orbital. For similar reasons the calculations are done for an internuclear distance of $R_e = 1.062$ Å, corresponding to the equilibrium distance of the $^2\Sigma^+$ Rydberg states and the NO^+ ion.[26]

It is important to note that the partial wave index l need not be equal to the single center expansion index l' in the case of molecular photoionization. For a central potential, $l = l'$. The nonspherical nature of the molecular ion potential causes a mixing between different l and l'. The dipole selection rules imply $l' = l_0 \pm 1$. This does not, however, imply that $l = l_0 \pm 1$. Which partial waves l are dominant depends on how l' and l are coupled via the molecular potential. For example, the 6σ orbital has predominantly $l_0 = 0$, and the 7σ $l_0 = 1$. Thus, for 6σ ionization we have $l' = 1$ while for 7σ ionization $l' = 0,2$. In spite of this difference, the odd-l partial waves are seen to be dominant in both cases. The strong $\Delta N = 0$ peak corroborates this as well. Thus, even though the bound state may have a strong atomic character, the low-energy photoelectron continuum can be, and often is, quite nonatomic.

The 7σ orbital is determined in the improved virtual orbital (IVO) approximation[27] using the fully relaxed core of the ion. The basis set used is given in Table I. The use of the fully relaxed ion core is justified by analyzing the relaxation effects for the $A\,^2\Sigma^+$ state. The direct SCF energy for the $A\,^2\Sigma^+$ state is $-129.076\,576$ a.u. IVO calculations with the $X\,^2\Pi$ ground state core and with the SCF $X\,^1\Sigma^+$ NO^+ ion core give $-129.038\,179$ and $-129.076\,419$ a.u., respectively. These results show that the ion core of the $A\,^2\Sigma^+$ state is nearly identical to the $X\,^1\Sigma^+$ NO^+ state. We have hence performed the IVO and photoelectron continuum calculations using the fully relaxed NO^+ as the frozen core. The calculated energy for the $D\,^2\Sigma^+$ state is $-129.038\,658$ a.u., corresponding to an excitation energy of 6.186 eV, compared with the experimental value of 6.582 eV.

III. RESULTS

In this section we will first address the $(2+1)$ one-color experiments of Ref. 15 via the $D\,^2\Sigma^+$ state of NO, and then the dependence of the rotational branching ratios on

TABLE I. Gaussian basis set used for the $A\,^2\Sigma^+$ and $D\,^2\Sigma^+$ Rydberg states: (10*s*6*p*1*d*) contracted to [6*s*4*p*1*d*] on nitrogen and oxygen, with an additional (7*s*7*p*) uncontracted basis set at the center of mass.

Center	Type	Exponent	Coefficient
N	*s*	5909.44	0.006 24
N	*s*	887.451	0.047 669
N	*s*	204.749	0.231 317
N	*s*	59.8376	0.788 869
N	*s*	19.9981	0.792 912
N	*s*	2.6868	0.323 609
N	*s*	0.7000	1.0
N	*s*	0.2133	1.0
N	*s*	0.1000	1.0
N	*p*	26.7860	0.038 244
N	*p*	5.9564	0.243 846
N	*p*	1.7074	0.817 193
N	*p*	0.5314	1.0
N	*p*	0.1654	1.0
N	*p*	0.0800	1.0
N	*d*	0.8000	1.0
O	*s*	7816.54	0.006 436
O	*s*	1175.82	0.048 924
O	*s*	273.188	0.233 819
O	*s*	81.1696	0.784 798
O	*s*	27.1836	0.803 381
O	*s*	3.4136	0.316 72
O	*s*	9.5322	1.0
O	*s*	0.9398	1.0
O	*s*	0.2846	1.0
O	*s*	0.1000	1.0
O	*p*	35.1832	0.040 023
O	*p*	7.9040	0.253 849
O	*p*	2.3051	0.806 842
O	*p*	0.7171	1.0
O	*p*	0.2137	1.0
O	*p*	0.0800	1.0
O	*d*	0.8000	1.0
CM	*s*	0.4000	1.0
CM	*s*	0.2000	1.0
CM	*s*	0.1300	1.0
CM	*s*	0.0500	1.0
CM	*s*	0.0250	1.0
CM	*s*	0.0100	1.0
CM	*s*	0.0050	1.0
CM	*p*	0.4000	1.0
CM	*p*	0.2000	1.0
CM	*p*	0.1300	1.0
CM	*p*	0.0500	1.0
CM	*p*	0.0250	1.0
CM	*p*	0.0100	1.0
CM	*p*	0.0050	1.0

the photoelectron kinetic energy for the (2 + 1′) REMPI via the $D\,^2\Sigma^+$ state and the (1 + 1′) REMPI via the $A\,^2\Sigma^+$ state.

The (2 + 1) REMPI experiments of Ref. 15 are one-color experiments via the 0–0 band of the *D*–*X* transition, rotationally resolved in the final ion state and rotationally assigned on the basis of data from Huber and Herzberg.[26] Photoelectron spectra are measured for the rotationally clean (only one J' contributing) $S_{21}(11.5)$ branch and the mixed $S_{11} + R_{21}(15.5)$ branch, with electron collection parallel and perpendicular to the polarization vector of the radiation. The photoelectron spectra show in both cases a pronounced $\Delta N = 0$ peak, reflecting a large odd partial wave character in the electronic continuum. The 7σ orbital has an angular decomposition of, 0.55% *s*, 99.20% *p*, 0.11% *d*, and 0.07% *f* character, in agreement with the results of Ref. 19. The bound-free dipole matrix elements, proportional to the $|r_{fi}^{l\lambda\mu}|^2$ of Eq. (4), are 0.0498, 0.0566, 0.0424, 0.0047, and 0.0002 for $l = 0$–4, respectively, in the $k\sigma$ channel and 0.0141, 0.2093, 0.0134, and 0.0019 for $l = 1$–4, respectively, in the $k\pi$ channel. This confirms the suggestion of Viswanathan *et al.*,[15] that the *p* wave is indeed present and strong, but also shows that the strongest ionization channel is the *d* wave of the $k\pi$ continuum. The total photoionization cross section is therefore dominated by the $k\pi$ channel. The rotationally unresolved, fixed nuclei, cross sections are 0.166 and 0.487 Mb for the $k\sigma$ and the $k\pi$ channel, respectively, in reasonable agreement with the earlier approximate calculations of Ref. 28. These calculated cross sections of the *D* state are about 50% of those obtained for the *A* state (see later). This trend is the exact opposite to that seen experimentally by Rottke and Zacharias,[12] who measured cross sections for the $A\,^2\Sigma^+$ state and the $D\,^2\Sigma^+$ state of 0.70 ± 0.09 and 6 ± 1 Mb, respectively (for specific rotational levels). We are at present unable to understand this discrepancy.

In Fig. 1, we compare the calculated photoelectron spectrum with the experimental spectrum[15] for the (2 + 1) REMPI via the rotationally clean $S_{21}(11.5)$ line of the 0–0 band of the *D*–*X* transition. The calculated results are convoluted with a Lorentzian detector function having a FWHM of 6 meV, a value chosen as representative of the actual experimental resolution. The calculated rotational branching ratios relative to the $\Delta N = -1$ signal are listed in Table II. The total calculated intensity for perpendicular detection for $\Delta N = -1$ is 7.1% of the corresponding parallel signal. The agreement between the theoretical and the experimental photoelectron spectra is quite good for parallel detection and excellent for perpendicular. The $\Delta N = 0$ signal is, as observed experimentally, significant in the parallel direction,

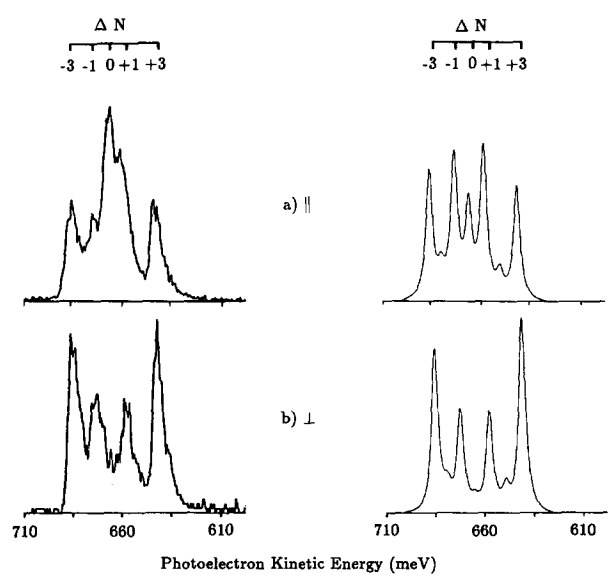

FIG. 1. Experimental (Ref. 15) (left-hand side) and calculated (right-hand side) photoelectron spectra with the laser tuned to the $S_{21}(11.5)$ line of the $D\,^2\Sigma^+ \leftarrow X\,^2\Pi$ transition of NO, for (a) laser light polarized parallel (||) to detection; (b) laser light polarized perpendicular (⊥) to detection.

TABLE II. (2 + 1) REMPI via the $D\,^2\Sigma^+$ state. Calculated rotational branching ratios for the $S_{21}(11.5)$ branch and the $S_{11}(15.5) + R_{21}(15.5)$ branch.

	Parallel (∥)		Perpendicular (⊥)	
ΔN	$S_{21}(11.5)$	$S_{11} + R_{21}(15.5)$	$S_{21}(11.5)$	$S_{11} + R_{21}(15.5)$
−3	0.763	0.489	1.974	1.516
−2	0.150	0.101	0.209	0.168
−1	1.000[a]	1.000[a]	1.000[a]	1.000[a]
0	0.590	0.401	0.093	0.096
+1	0.936	0.965	1.009	1.016
+2	0.158	0.110	0.186	0.185
+3	0.857	0.560	1.643	1.765

[a] Normalized to this line.

but very small (nonobservable) in the perpendicular direction, demonstrating the sharpness around $\theta = 0°$ of the angular distribution for the $\Delta N = 0$ peak. The $P(\theta)$ of Eq. (3), the angular distribution of the photoelectrons, can be expanded in Legendre polynomials $P_L[\cos(\theta)]$ as

$$P(\theta) = \sum_{L=0,2,\ldots}^{L_{\max}} \beta_L \cdot P_L[\cos(\theta)], \tag{5}$$

where L_{max} in these weak intensity studies is determined by the order of the process. For the $\Delta N = 0$ signal the normalized β parameters are $\beta_0 \equiv 1.000$, $\beta_2 = 1.899$, $\beta_4 = 0.104$, and $\beta_6 = 0.003$.

Mixed branches, such as the $S_{11}(15.5) + R_{21}(15.5)$ branch, can be treated as individual ionization channels, although indistinguishable in the photoelectron spectrum. They can be incoherently added with the proper weighting, as determined by Eq. (2). The relative weights [the B factor of Eq. (2)] are 0.012 20 and 0.004 92, as determined by Halpern,[23] for the $S_{11}(15.5)$ and the $R_{21}(15.5)$ branches, respectively. The two individual branches are calculated as outlined above. In Fig. 2, we compare the experimental and the calculated photoelectron spectra for the mixed $S_{11} + R_{21}(15.5)$ branch. The calculated intensities are again convoluted with a Lorentzian detection function with a FWHM of 6 meV, and the relative branching ratios are listed in Table II. The $\Delta N = 0$ signal is found to be strong in the parallel direction, although less pronounced in the calculated spectrum than in the experimental spectrum. The agreement is seemingly far better in the perpendicular direction. The calculated $\Delta N = 0$ signal is very small, consistent with the experimental observation. The normalized β parameters for the angular distribution of the $\Delta N = 0$ signal are $\beta_0 \equiv 1.000$, $\beta_2 = 1.796$, $\beta_4 = 0.099$, and $\beta_6 = -0.001$. The total strength of the perpendicular $\Delta N = -1$ signal is calculated to be about 18.3% of the corresponding parallel signal.

An important dynamical aspect of the photoionization is the energy dependence of the $r_{fi}^{l\lambda\mu}$ matrix elements of Eq. (4). In the one-color experiments of Ref. 15 the final photoelectron kinetic energies span a range of about 1.0 eV for the REMPI via the different Rydberg states, i.e., from ~1.7 eV for (1 + 1) REMPI via the $A\,^2\Sigma^+$ state to ~0.7 eV for the (2 + 1) REMPI via the $D\,^2\Sigma^+$ state. The anomalous

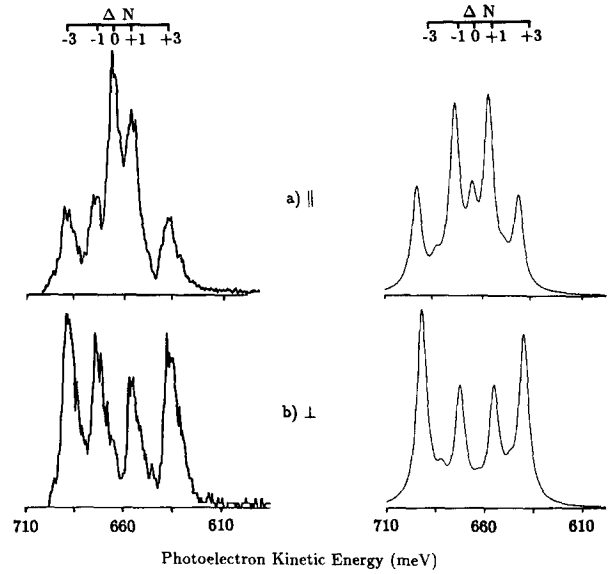

FIG. 2. Same as Fig. 1, but for the mixed $R_{21}(15.5) + S_{11}(15.5)$ branch.

$\Delta N = 0$ peaks, observed in the $D\,^2\Sigma^+$ REMPI experiments, can therefore be a possible consequence of this energy dependence. To investigate this, we have calculated the rotational branching ratios for a range of photoelectron kinetic energies (0.5, 1.0, 1.5, and 2.0 eV). In Fig. 3, we show the rotational branching ratios for the (2 + 1′) REMPI via the $D\,^2\Sigma^+ S_{21}(11.5)$ branch and of the (1 + 1′) REMPI via the $A\,^2\Sigma^+ R_{22}(21.5)$ branch as a function of the photoelectron kinetic energy. The branching ratios for the D state show a

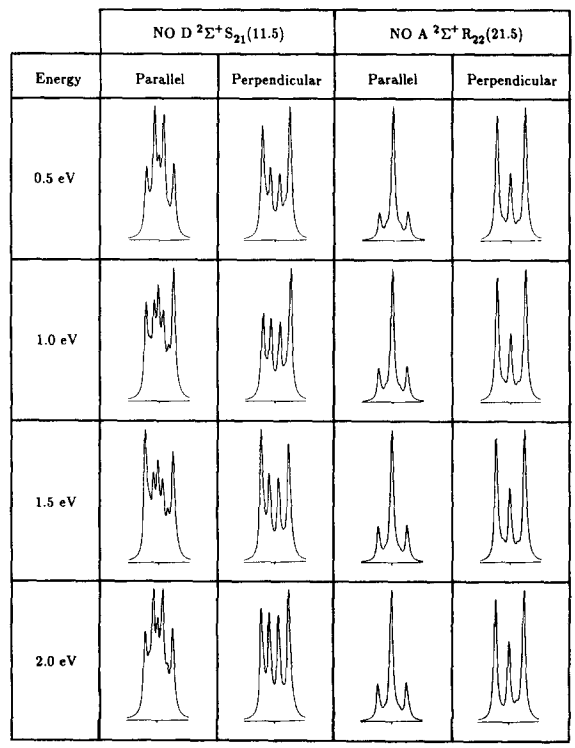

FIG. 3. Photoelectron spectra as a function of photoelectron kinetic energy, for the $S_{21}(11.5)$ branch of the $D\,^2\Sigma^+$ state, and for the $R_{22}(21.5)$ branch of the $A\,^2\Sigma^+$ state. Total length of the abscissa corresponds to 100 meV.

pronounced energy dependence for both directions of detection, whereas the branching ratios for the A state are rather insensitive to photoelectron kinetic energy. This may result from the fact that the A state ionization into the $l = 1$ partial wave does not require a nonspherical potential whereas for the D state this channel is a direct consequence of angular momentum coupling in the continuum, i.e., $l' \neq l$ mixing. This behavior in the D state photoionization is expected to be strongly energy dependent. The total cross sections (rotationally unresolved, fixed nuclei) show a similar dependence on the photoelectron kinetic energy, i.e., the D state cross sections are 0.806 (0.5 eV), 0.450 (1.0 eV), 0.320 (1.5 eV), and 0.273 Mb (2.0 eV), whereas the A state cross sections are, 1.188 (0.5 eV), 1.199 (1.0 eV), 1.172 (1.5 eV), and 1.122 Mb (2.0 eV).

IV. CONCLUSIONS

We have presented results for the rotationally resolved photoelectron spectra resulting from a $(2 + 1)$ one-color REMPI of NO via the rotationally clean $S_{21}(11.5)$ and mixed $S_{11}(15.5) + R_{21}(15.5)$ branches of the 0–0 transition in the D–X band. The calculations were done in the fixed-nuclei frozen core approximation, where the frozen core of the $D\,^2\Sigma^+$ Rydberg state is taken to be the $X\,^1\Sigma^+$ ground state of NO^+. The resulting photoelectron spectra, convoluted with a Lorentzian detection function, agree qualitatively with the experimental results of Viswanathan *et al.*,[15] and support their conclusion, that the nonspherical nature of the molecular potential creates a substantial l mixing in the continuum, which in turn leads to the intense $\Delta N = 0$ peak. We have furthermore investigated the rather strong photoelectron energy dependence of the rotational branching ratios of the $D\,^2\Sigma^+\,S_{21}(11.5)$ line, and compared this to the weak energy dependence of the $A\,^2\Sigma^+\,R_{22}(21.5)$ line. We attribute this behavior to differences in the bound states and the different parts of the electronic continuum probed. This work illustrates the ability of *ab initio* calculations to unravel the subtle features in the photoionization dynamics for rotationally clean and mixed branches. The present work does not include effects of autoionization, high intensities, nor the possible alignment deteriorating effects.

ACKNOWLEDGMENTS

This material is based on research supported by the National Science Foundation under Grant NO. CHE-8521391, AFOSR under Grant NO. 87-0039, and the Office of Health and Environmental Research of DOE (DE-FGO3-87-ER60513), and by NASA-Ames Cooperative Agreement NO. NCC2-319. Work done by S.N.D. was performed under the auspices of the U. S. Department of Energy by Lawrence Livermore National Laboratory under Contract No. W-7405-Eng-48. H.R. gratefully acknowledges the support from the Danish Natural Science Research Council.

[1] P. Chen, J. B. Pallix, W. A. Chupka, and S. D. Colson, J. Chem. Phys. **86**, 516 (1987).
[2] A. Sur, C. V. Ramana, W. A. Chupka, and S. D. Colson, J. Chem. Phys. **84**, 69 (1986).
[3] D. Normand, C. Cornaggia, and J. Morellec, J. Phys. B **19**, 2881 (1986).
[4] T. M. Orlando, L. Li, S. L. Anderson, and M. G. White, Chem. Phys. Lett. **129**, 31 (1986).
[5] S. L. Anderson, G. D. Kubiak, and R. N. Zare, Chem. Phys. Lett. **105**, 22 (1984).
[6] S. T. Pratt, P. M. Dehmer, and J. L. Dehmer, J. Chem. Phys. **78**, 4315 (1983).
[7] S. T. Pratt, P. M. Dehmer, and J. L. Dehmer, J. Chem. Phys. Lett. **105**, 28 (1984).
[8] W. Meier, H. Rottke, H. Zacharias, and K. W. Welge, J. Chem. Phys. **83**, 4360 (1985).
[9] J. E. Polland, D. J. Trevor, J. E. Reutt, Y. T. Lee, and D. A. Shirley, J. Chem. Phys. **77**, 34 (1982).
[10] H. Zacharias, R. Schmeidl, and K. H. Welge, Appl. Phys. **21**, 127 (1980).
[11] J. P. Booth, S. L. Bragg, and G. Hancock, Chem. Phys. Lett. **113**, 509 (1985).
[12] H. Rottke and H. Zacharias, J. Chem. Phys. **83**, 4831 (1985).
[13] J. C. Miller and R. N. Compton, J. Chem. Phys. **84**, 675 (1986).
[14] W. G. Wilson, K. S. Viswanathan, E. Sekreta, and J. P. Reilly, J. Phys. Chem. **88**, 672 (1984).
[15] K. S. Viswanathan, E. Sekreta, E. R. Davidson, and J. P. Reilly, J. Phys. Chem. **90**, 5078 (1986).
[16] K. S. Viswanathan, E. Sekreta, and J. P. Reilly, J. Phys. Chem. **90**, 5658 (1986).
[17] See, for example, K. Müller-Dethlefs, M. Sander, and E. W. Schlag, Chem. Phys. Lett. **112**, 291 (1984).
[18] S. N. Dixit and V. McKoy, Chem. Phys. Lett. **128**, 49 (1986).
[19] K. Kaufmann, C. Nager, and M. Jungen, Chem. Phys. **95**, 385 (1985).
[20] S. N. Dixit, D. L. Lynch, V. McKoy, and W. M. Huo, Phys. Rev. A **32**, 1267 (1984).
[21] H. Rudolph, S. N. Dixit, V. McKoy, and W. M. Huo, Chem. Phys. Lett. **137**, 521 (1987).
[22] S. N. Dixit and V. McKoy, J. Chem. Phys. **82**, 3546 (1985).
[23] J. B. Halpern, H. Zacharias, and R. Wallenstein, J. Mol. Spectrosc. **79**, 1 (1980).
[24] L.T. Earls, Phys. Rev. **48**, 423 (1935).
[25] R. R. Lucchese, G. Raseev, and V. McKoy, Phys. Rev. A **25**, 2572 (1982).
[26] K. P. Huber and G. Herzberg, *Constants of Diatomic Molecules* (Van Nostrand Reinhold, New York, 1979).
[27] W. J. Hunt and W. A. Goddard III, Chem. Phys. Lett. **24**, 464 (1974).
[28] P. Cremaschi, Chem. Phys. Lett. **83**, 106 (1981).